metry is exhibited by the Juan de Fuca Ridge (*8*). Three profiles across the ridge are shown in Fig. 4; they are at 45-km intervals along the ridge. In Fig. 3 the central profile is shown together with its mirror image to demonstrate the symmetry. This suggests a quiet growth for the ridge, and it is possibly significant that no active submarine volcanism has been reported from this area despite the fact that the ridge is presumed to be active because of the occurrence of recent earthquakes along the bounding transform faults (*8*). Symmetry of ridge profiles might be sought elsewhere. As with correlation of magnetic anomalies on adjacent profiles, the symmetry of the anomalies about the axis of a ridge is probably much less obvious from profiles than from a detailed survey.

It is becoming increasingly apparent that both the linearity of oceanic, magnetic anomalies and the steep gradients which bound them are obvious from a detailed magnetic survey but much more difficult to see from comparatively random profiles. Even the marked linearity of the anomalies over the Juan de Fuca Ridge is not necessarily obvious from adjacent profiles across it. Although profiles *a* and *b* in Fig. 4 correlate well, their correlation with profile *c* is not so good, and one might easily not anticipate the pronounced "grain" of the survey map (*1*). We should therefore like to reiterate the recent plea by Peter and Stewart (*1*) that magnetic surveys are of so much greater value than random profiles. Aeromagnetic surveys would appear to be perfectly adequate. It has been known for several years, but more convincingly established recently (*1, 11*), that the magnetic anomalies are, in general, quite unrelated to the bathymetry except over isolated seamounts or apparent transcurrent faults [all of which are, possibly, transform faults (9)].

F. J. VINE*
Department of Geodesy and
Geophysics, University of Cambridge,
Cambridge, England

J. TUZO WILSON
Institute of Earth Sciences, University
of Toronto, Toronto, Canada

References and Notes

1. R. G. Mason, *Geophys. J.* **1**, 320 (1958); V. Vacquier, A. D. Raff, R. E. Warren, *Bull. Geol. Soc. Am.* **72**, 1251 (1961); R. G. Mason and A. D. Raff, *ibid.* **72**, 1259 (1961); A. D. Raff and R. G. Mason, *ibid.* **72**, 1267 (1961); G. Peter and H. B. Stewart, *Nature* **206**, 1017 (1965).
2. F. J. Vine and D. H. Matthews, *Nature* **199**, 947 (1963).
3. A. Holmes, *Trans. Geol. Soc. Glasgow* **18**, 559 (1928–29); H. H. Hess, "History of ocean basins," in *Petrologic Studies*, A. E. J. Engel *et al.*, Eds. (Geological Soc. of America, New York, 1962), p. 599.
4. H. W. Menard, *Marine Geology of the Pacific* (McGraw-Hill, New York, 1964).
5. H. H. Hess, "Mid-ocean ridges and tectonics of the sea floor," in *Colston Volume on Marine Geology* (Univ. of Bristol, Bristol, England, in press).
6. A. Cox, R. R. Doell, G. B. Dalrymple, *Nature* **198**, 1049 (1963).
7. ———, *Science* **144**, 1537 (1964).
8. J. T. Wilson, *Science*, this issue.
9. ———, *Nature* **207**, 343 (1965).
10. C. A. Whitten, *Trans. Am. Geophys. Union* **29**, 318 (1948).
11 J. R. Cann and F. J. Vine, *Phil. Trans. Roy. Soc. Lond. Ser. A*, in press.
12. G. Bodvarsson and G. P. L. Walker, *Geophys. J.* **8**, 285 (1964).
13. A. Cox, R. R. Doell, G. Thompson, *A Study of Serpentinite* (NAS–NRC Publ. No. 1188, 1964), p. 49.
14. J. M. Ade-Hall, *Geophys. J.* **9**, 85 (1964).
15. For all three models in Fig. 1 the intensity of the earth's field has been taken as 54,000 gamma, its dip as +66°, and the magnetic bearing of the profile as 087°, that is, as for the Juan de Fuca Ridge (46°30′N, 129°30′W). Normal or reverse magnetization is with respect to an axial dipole vector; axial dipole dip taken as +65°. Effective susceptibility of the blocks, ±0.0025, except for the central block, +0.005 (1 gamma = 10^{-5} oersted).
16. J. R. Heirtzler, *Tech. Rept. No. 2* (Lamont Geol. Observ., New York, 1961).

17. We thank Sir Edward Bullard, J. R. Cann, H. H. Hess, R. G. Mason, and D. H. Matthews for valuable suggestions, and Sue Vine for preparing the manuscript. The paper was written while one of us (J.T.W.) was a guest of the department of geodesy and geophysics, University of Cambridge.

* Present address: Department of Geology, Princeton University, Princeton, N.J.

21 June 1965

■

Radioactivity: Distribution from Cratering in Basalt

Abstract. *Samples of airborne and ground-deposited debris produced by an experiment in nuclear excavation were analyzed to determine the fate of various radioactive nuclides. A few tenths percent of the nonvolatile species and 10 to 20 percent of the volatile species escaped beyond the immediate vicinity of the crater.*

Suggested uses for nuclear excavation include the production of railroad cuts, mines, and harbors. Its first major use may be in constructing a new transisthmian canal. Very little information is available concerning the release of radioactivity, one of its most serious technical and political problems. The most relevant data come from the Danny Boy experiment at the Atomic Energy Commission's Nevada Test Site at 1015 hours P.S.T., 5 March 1962; ground zero was at 37°06′39.79″N, 116°21′53.82″W (*1*).

The Danny Boy event was an underground nuclear explosion designed to produce a crater in hard rock (basalt). A 0.43-kiloton device, detonated 33.5 m below the surface, formed a crater 18.9 m deep and 65.2 m in diameter (*2*). The cloud from the detonation grew rapidly to a width of about 900 m and a height of 300 m; after about 3 minutes growth was controlled primarily by ordinary atmospheric dispersion processes. At the time of detonation, winds were 22 km/hr from 168° azimuth at the surface and 50 km/hr from 190° 1100 m above ground. On 6 March there were wind gusts in the morning, with 1.22 cm of precipitation during the day (*2, 3*). Much of the total radioactivity produced was trapped in and below the

Table 1. Results of chemical analyses of samples from fallout trays, expressed as *J* values: disintegrations of nuclide *i*. J_i, disintegrations per minute (of nuclide *i*) per square meter, divided by the field reading in millirads per hour. In recording *J* values, the factor shown at the head of each column was omitted; to obtain original values, multiply each tabulation by the appropriate factor.

Station, distance* (m)	Field reading†	*J* value										
		Sr^{89} (10^{5})	Sr^{90} (10^{3})	Zr^{95} (10^{5})	Mo^{99} (10^{6})	Cs^{136} (10^{4})	Cs^{137} (10^{3})	Ba^{140} (10^{6})	Ce^{141} (10^{5})	Ce^{144} (10^{4})	Nd^{147} (10^{5})	Eu^{156} (10^{4})
E-1, 762	48	1.9	2.2	1.4	5.8	6.3	3.7	2.9	8.1	3.5	5.3	2.3
T-17, 762	22	0.62	0.62	0.81	2.6	2.9	1.1	1.2	3.5	1.7	2.2	0.93
E-3, 1524	17	6.5	6.3	2.0	6.1	11	9.8	6.1	12	4.1	5.2	3
E-5, 2286	6	3.7	2.8	1.2	3.8	7.1	7.6	3.7	7.2	2.3	3.2	1.4
E-7, 3048	3	6.6	5.2	2.7	11	12	12	1	11	4.1	8.6	3.4
W-11, 3048	10	4.0	3.2	3.1	9.2	15	7.1	5.7	12	4.8	7.5	4.4
X-22, 5182	8	3.1	2.5	2.7	8.5	9.8	5.2	4.2	11	5.3	8.1	3.3
Y-20, 7620	0.6	3.9	2.2	0.73	2.7	3.5	9.7	2.5	4.5	1.5	2	1
Y-26, 7620	.4	0.22	0.29	.16	1.0	1.2	0.52	0.27	9.3	3.4	0.48	0.29
Average J_i		3.4	2.8	1.6	5.6	7.6	6.3	3.1	8.7	3.4	4.7	2.2

* From point of detonation. † Millirads per hour, 1500 hours 6 March.

Table 2. Percentages of various nuclides in the fallout pattern. Abbreviations: d/min, disintegrations per minute.

Nuclide	Fallout produced (10^{14} d/min)	Fallout beyond 762 m	
		At t_0 (10^{13} d/min)	Percentage
Sr^{89}	106	7.4	0.70
Sr^{90}	0.665	0.061	.92
Zr^{95}	195	3.5	.18
Mo^{99}	6100	120	.20
Cs^{136}	22.1	1.7	.77
Cs^{137}	1.67	0.14	.84
Ba^{140}	1190	68	.57
Ce^{141}	438	19	.43
Ce^{144}	42	0.74	.18
Nd^{147}	570	10	.18
Eu^{156}	29.4	0.48	.16
Pu^{239}			.16

crater, but some escaped. The radiochemical program attempted to measure the amount that escaped and, as far as possible, to trace the fate of the escaped material. Samples for radiochemical analysis were obtained by collection of fallout and by cloud sampling with filter-equipped aircraft. Results from the two types of samples are discussed separately.

Before the detonation, an array of fallout collectors and radiation-survey points was laid out in the downwind sector (Fig. 1). The radiation measurements (*3*) were made by survey teams from the U.S. Army Nuclear Defense Laboratory. The fallout trays (*4*) were collected on 5 and 6 March after the explosion; many of those collected on 6 March were snow-covered or wet. The collected trays were processed (*4*) to remove radioactive debris, and selected samples were sent to the laboratory for radiochemical analysis (*5*).

One object of the fallout study was to determine the total amounts of individual nuclides in the pattern. Since only a few samples were analyzed radiochemically, it was not possible to make a good integration from these data alone; for this reason the field readings of radiation were used for the integration. The radiochemical analyses were then related to the field readings to derive the total amounts of individual nuclides in the fallout.

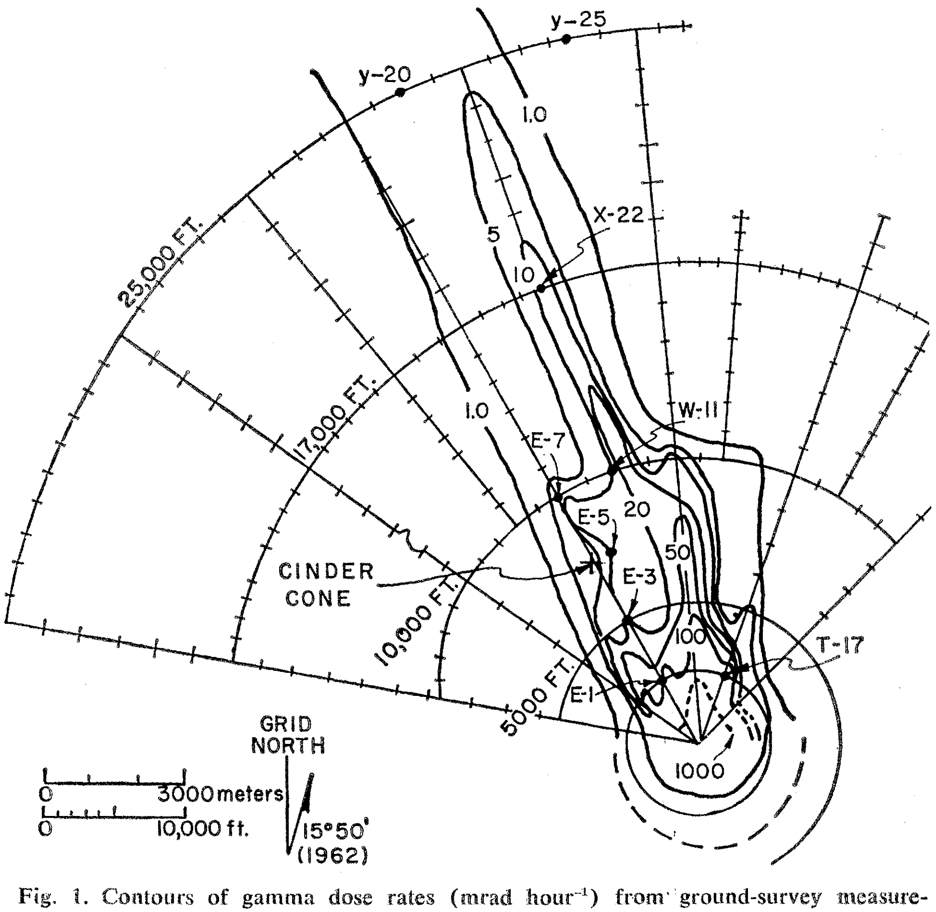

Fig. 1. Contours of gamma dose rates (mrad hour^{-1}) from ground-survey measurements on D+1 (*2*). Sampling and survey points are indicated.

The data used for integrating the fallout pattern (Fig. 1) were the field readings of radiation obtained (*3*) at about 1500 hours on 6 March (D + 1). Before integration, all readings were corrected to 1500 hours on D + 1, with $t^{-1.3}$ as the decay correction. The average value of the field as a function of distance from ground zero is shown in Fig. 2; each point on the curve was obtained by averaging the field intensities at that distance over 360°. The equation for the line drawn through the points of Fig. 2 is

$$A(r) = 3.7 \times 10^8 \; r^{-2.47}$$

where $A(r)$ is the average value of the field, in millirads per hour, at r, and r is the distance from ground zero in meters. The total activity Q (mrad hour^{-1} m^2) between r_1 and r_2 is given by

$$Q = 2\pi \int_{r_1}^{r_2} A(r) \, r dr$$

$$= 2\pi \int_{r_1}^{r_2} 3.7 \times 10^8 \; r^{-1.47} \, dr$$

$$= 4.9 \times 10^9 \left[r^{-0.47} \right]_{r_2}^{r_1}.$$

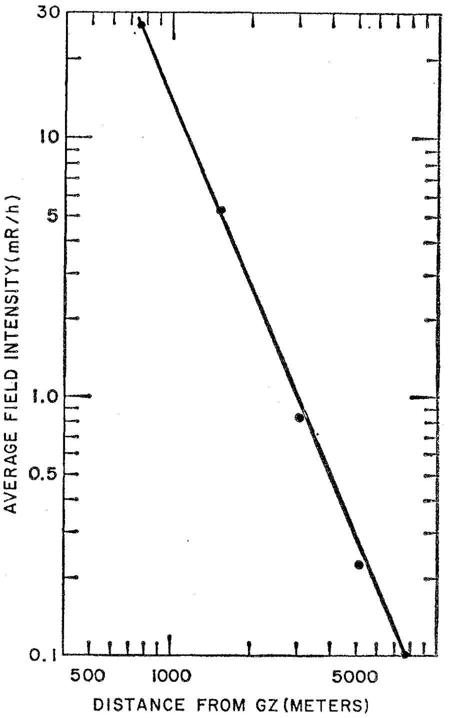

Fig. 2. Average field intensity versus distance from ground zero (mrad hour^{-1} at 1500 hours on D+1).

The survey extended from 762 to 7620 m; the value of Q between these limits, Q_{7620}, is 1.45 × 10^8 mrad hour^{-1} m^2. If $A(r)$ can be extrapolated to infinity, the value of Q between the limits 762 m and ∞, Q_∞, is 2.2 × 10^8 mrad hour^{-1} m^2. According to this extrapolation, only about one-third of the fallout is beyond the measured region.

The results of the radiochemical analyses of the fallout samples, along

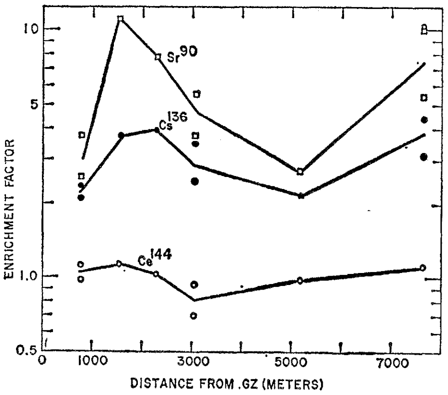

Fig. 3. Enrichment factors in fallout samples, relative to Nd^{147}, plotted against distance from ground zero.

with the field readings taken at the sources of the samples, are summarized in Table 1. The measured disintegration rates of each nuclide are not given, but can be readily obtained from the field reading and J_i, the ratio of the activity per square meter of nuclide i in the sample to the field reading; J_i is not a constant. However, since the ratio does not appear to have a consistent trend with distance, the average value was used as representative of the entire pattern (*6*).

The geometric area of the collecting trays was 0.372 m^2; it was assumed that this was equivalent to 0.372 m^2 of ground, but because of perturbations caused by the tray this assumption was probably not valid (*7*). The variation of the J_i values in Table 1 probably indicates the degree of uncertainty in this assumption.

To determine the total amount of a nuclide in the fallout pattern beyond 762 m the average value of J_i was multiplied by Q_∞. These totals are tabulated in Table 2 and compared with the amounts produced in the nuclear explosion. Because of the inconsistent values of J_i and the errors introduced by the integration, these totals and percentages are uncertain by perhaps a factor of two; the relative values, however, are considerably more reliable. The percentage of the total activity produced that lies in the fallout pattern beyond 762 m is between 0.1 and 1 percent in all cases. The data on plutonium distribution are not included in Table 1, but the pattern is very similar to those for Ce^{144}, Nd^{147}, and Eu^{156}.

Table 3 lists the data relating to fractionation in the fallout pattern; the numbers, which we have called enrichment factors, are measures of enrichment of the nuclides relative to Nd^{147}; for example, for Sr^{90} the entries in the table are

$$\frac{\text{Atoms Sr}^{90}\text{ in sample}}{\text{Atoms Nd}^{147}\text{ in sample}} \times \frac{\text{atoms Nd}^{147}\text{ produced}}{\text{atoms Sr}^{90}\text{ produced}}$$

In other words, a Sr^{90} enrichment factor is the fraction of the total Sr^{90} collected in the sample divided by the fraction of the total Nd^{147}. If Sr^{90} has not separated from Nd^{147} in a particular sample, the entry for Sr^{90} for that sample is 1.0. A value greater than unity indicates an enrichment in Sr^{90} relative to Nd^{147}; a value less than unity, a depletion.

The enrichment factors plotted in Fig. 3 against distance from ground zero were picked to show the behavior of three groups of nuclides: (i) "volatile" nuclides such as Sr^{89}, Sr^{90}, Cs^{137}, and Ba^{140}; (ii) nonvolatile nuclides such as Ce^{144}, Nd^{147}, and Zr^{95}; and (iii) the intermediate group such as Cs^{136} and Ce^{141}.

Table 3. Enrichment factors, relative to Nd^{147}, in fallout samples.

Station	Sr^{89}	Sr^{90}	Zr^{95}	Mo^{99}	Cs^{136}	Cs^{137}	Ba^{140}	Ce^{141}	Ce^{144}	Eu^{156}
E-1	2.2	3.7	0.84	1.1	2.1	2.4	2.9	2.3	0.97	0.99
T-17	1.7	2.6	1.2	1.1	2.3	1.8	3.0	2.5	1.1	0.97
E-3	7.5	11	1.2	1.1	3.7	6.5	6.3	3.6	1.1	1.3
E-5	7.1	7.8	1.1	1.1	3.9	8.2	6.2	3.4	1.0	1.0
E-7	4.8	5.5	1.0	1.2	2.5	4.8	0.62	2.0	0.70	0.98
W-11	3.3	3.7	1.3	1.2	3.5	3.3	4.0	2.4	0.93	1.4
X-22	2.3	2.7	1.1	1.0	2.2	2.3	2.8	2.1	0.98	0.96
Y-20	12	10	1.2	1.3	3.1	17	6.9	3.4	1.1	1.2
Y-26	2.7	5.4	1.0	2.0	4.4	3.8	3.0	29*	10*	1.4

* These values appear anomalous despite careful checking; apparent discrepancy may result from the low activity level of sample Y-26.

Table 4. Enrichment factors, relative to Nd^{147}, in aircraft samples.

Isotope	Mean time of sampling after detonation (minutes)			
	8	15	47	138
Sr^{89}	142	236	428	754
Sr^{90}	90	137	240	421
Y^{91}	32	45	77	130
Zr^{95}	1.0	1.2	1.2	2.0
Zr^{97}	0.91	0.99	1.0	1.1
Mo^{99}	.98	1.1	1.1	1.2
Ag^{111}	3.6	4.0	4.7	5.7
Cd^{115}	4.6	5.2	6.3	7.7
Cs^{136}	3.4	3.6	5.0	6.2
Cs^{137}	125	212	425	755
Ba^{140}	38	54	91	155
Ce^{141}	4.6	5.7	8.1	11
Ce^{144}	1.0	1.2	1.3	3.7
Sm^{153}	2.1	2.5	2.2	2.4
Eu^{156}	0.94	1.1	1.0	1.2

The mean times of four samplings of particulate matter by airborne filters were 8, 15, 47, and 138 minutes after detonation. The filter medium used was IPC-1478 filter paper; the air velocity was about 13 m/sec. Under these conditions particles of about 1-μ diameter or larger are collected with nearly 100 percent efficiency; efficiency then decreases with size, with 0.2-μ particles being collected with about 50-percent efficiency. The results of radiochemical analyses of these samples, expressed as enrichment factors relative to Nd^{147}, appear in Table 4 and in Fig. 4, *a* and *b*. The volatile species are much more enriched in these aircraft samples than in the fallout samples; the relative enrichments decrease with decreasing half-life of the rare-gas precursors. The total amount of each measured nuclide in the cloud can be estimated from knowledge of the cloud volume relative to the volume swept by the sampler. Photographs at 3 minutes (*8*) show the cloud to be 300 m high and 900 m in diameter, with a volume of 1.90×10^8 m^3. No photographs were taken after 3 minutes, but if lateral diffusion had occurred the diameter is calculated (*9*) to have been 2400 m at 8 minutes, with the height remaining 300 m; these dimensions correspond to a volume of 1.35×10^9 m^3.

The effective collecting area of the filter unit was 5.26×10^{-2} m^2. If it is assumed that the calculated cloud volume is correct, the fraction of the cloud debris collected during the 8-minute sampling was $5.26 \times 10^{-2} \times 2400/1.35 \times 10^9$, or 9.35×10^{-8}. This fraction can be combined with the disintegrations per minute in the sample and with the total disintegrations per minute produced to calculate the percentage of any measured isotope found in the cloud at 8 minutes. For Cs^{137}, the most volatile species measured, the amount in the cloud is 13 percent; for Nd^{147}, one of the least volatile, 0.11 percent. The percentage

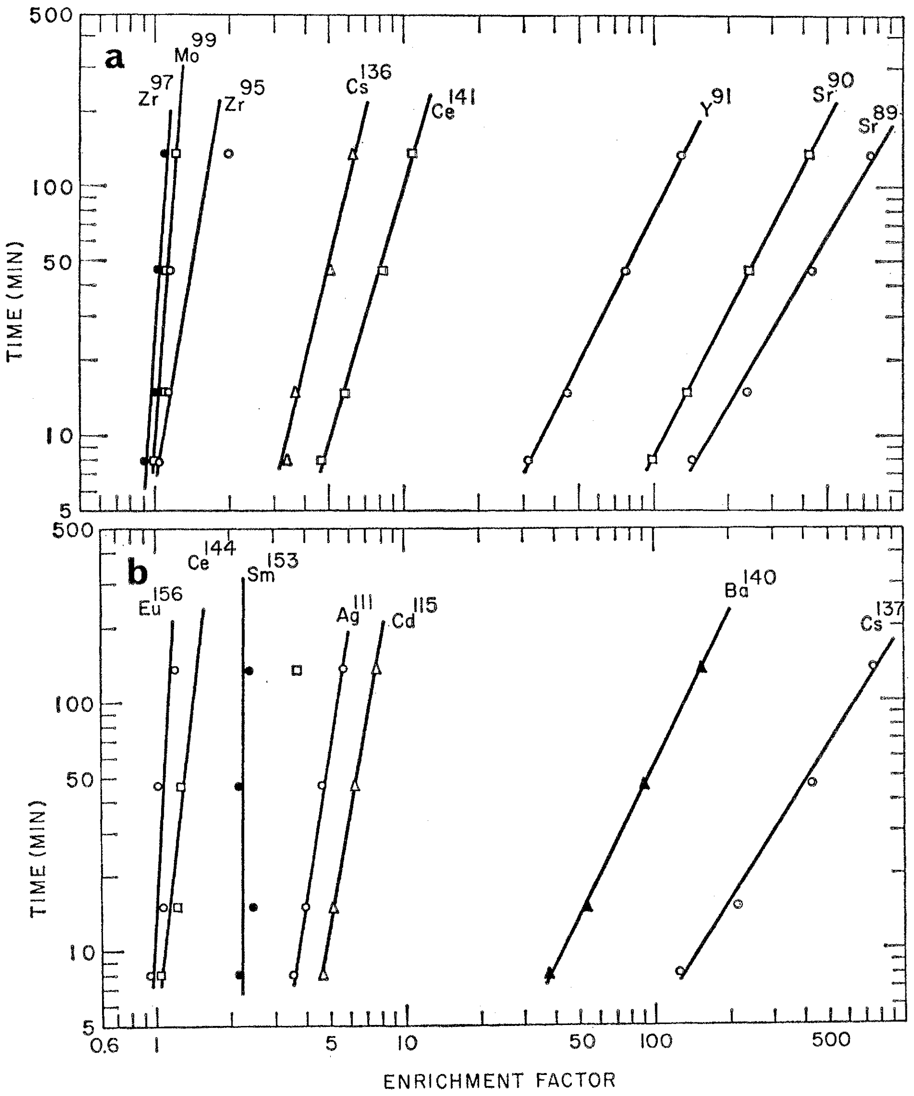

Fig. 4. (*a* and *b*) Enrichment factors in aircraft samples, relative to Nd^{147}, plotted against time after burst.

of any of the other measured fission products in the cloud at 8 minutes can be estimated by multiplying its enrichment factor (Table 4) by 0.11.

The principal error in these percentages lies in the estimate of the fraction of cloud debris collected in the sample. The cloud volume used in the calculation is probably an upper limit, which would lead to high values of the percentages in the cloud. The effective volume of cloud sampled by the sampling airplane could be in error in either direction: sampling a region of abnormally high or low concentration would give proportionately high or low results. We feel that the figures given are more likely to be high than low. The relative amounts of various species in the cloud are much more precise than the absolute values, just as in the fallout samples.

Although at 8 minutes the cloud was about 3300 m from ground zero, calculations by Knox (*9*) indicate that the activity in the upper part of the cloud (where the sample was taken) at 8 minutes is not deposited in the measured fallout area, but rather falls well beyond it; the average deposition distance for this material is 37 km from ground zero. Thus one cannot make a simple comparison of the composition of this sample with that of the fallout samples.

Thus the two methods of sampling—collection of close-in fallout and aircraft sampling—give complementary information. For nonvolatile species such as Nd^{147}, the amount remaining in the cloud at 8 minutes (about 0.1 percent) is not inconsistent with the total amount in the integrated fallout pattern (about 0.2 percent). Thus a reasonable conclusion is that about 0.2 percent of the total nonvolatile species produced escaped, and that most of this was deposited as close-in fallout.

For the volatile species (or species with volatile precursors) such as Cs^{137}, the situation is quite different: close-in fallout is somewhat enriched in such nuclides (Table 3), the amount of Cs^{137}, for example, being about 0.9 percent in contrast with 0.2 percent for Nd^{147}. The cloud samples, however, are greatly enriched in the volatile species (Table 4); amounts remaining in the cloud at 8 minutes are not at all consistent with the totals in the fallout pattern. For example, 13 percent of the Cs^{137} produced is in the cloud at 8 minutes, while only 0.9 percent is in the integrated fallout pattern. In other words, the volatile species do not fall out nearly as quickly as the nonvolatile ones, a fact borne out by some of the extremely large enrichment factors in the later aircraft samples. Total amounts of volatile species that escaped must be estimated from the cloud-sample measurements and not from the fallout samples.

In conclusion, it appears that a few tenths of 1 percent of the nonvolatiles and 10 to 20 percent of the more-volatile species were released. No data were obtained on permanent gases or I^{131}. A large fraction of the nonvolatiles fell within 15 km, whereas most of the volatiles did not. These figures apply only to this experiment, of course; there will be variation with depth of burial of the explosive and with the nature of the surrounding earth. The common practice of describing the radioactive release from a partially contained nuclear detonation in terms of "fraction out" or "percentage vented" is meaningless unless applied to specific isotopes.

NORMAN A. BONNER
JOHN A. MISKEL

Chemistry Department,
Lawrence Radiation Laboratory,
University of California, Livermore

References and Notes

1. In the Timber Mountain quadrangle, according to the Army Map Service.
2. M. Nordyke and W. Wray, "Results from a nuclear cratering detonation in basalt," *Lawrence Radiation Lab. Rept. UCRL-6999, Revision 2* (Univ. of California, Livermore, 1963).
3. W. G. Powell and E. F. Wilsey, *On-Site Fallout from a Partially Contained Nuclear Burst in a Hard Rock Medium, POR-1819* (U.S. Army Nuclear Defense Lab., Maryland, 1963).
4. E. M. Romney, J. W. Neel, G. M. LeRoy, A. J. Steen, K. H. Larson, *Amer. Ind. Hyg. Assoc. J.* **20**, 267 (1959).
5. Radiochemical analyses performed by the U.S. Air Force.
6. Some calculations were made based on the measured ratio of activity to field reading at each distance. The total amount of the nuclide deposited was then obtained by numerical integration. Differences between these results and those obtained by use of the average ratio were not significant in view of the uncertainties involved.

7. The fallout trays were low-sided flat pans covered to a depth of about 1.3 cm with polyethylene spheres 0.63 cm in diameter. Because most of the particles are traveling at extremely low angles at the moment of collection, orientation of the tray and the micrometeorology of its vicinity are very important; it is unlikely that the geometric area of the tray is equivalent to that of the ground. Moreover, the polyethylene balls complicate the chemistry by making difficult the removal of the collected material. We shall not use this type of collector again.
8. B. M. Carder, L. P. Donovan, D. J. Barnes, *Project Danny Boy—Surface Phenomena Photography, POR-WT1812* (AEC, Oak Ridge, Tenn., 1963).
9. J. Knox, private communication, 1964.
10. Sponsored by the AEC.

9 August 1965

Exchange of Carbon-Bound Hydrogen Atoms ortho to the Hydroxyl Group in Tyrosine

Abstract. *The carbon-bound hydrogen atoms of tyrosine that exchange with solvent protons in strongly acid solutions at about 100°C are not the methylene hydrogen atoms but a pair on the aromatic ring. Of the two pairs of protons on the aromatic ring, observed in the proton magnetic resonance spectra, the pair at higher field undergoes exchange in 2.4*N *DCl at 100°C. Other hydrogen atoms, attached either to aliphatic or aromatic carbon atoms, exhibit no noticeable exchange under the same conditions. From a chemical-shift analysis the exchanging protons are assigned as those* ortho *to the hydroxyl group on the aromatic ring.*

Study of hydrogen-isotope exchange has been used to acquire information concerning the secondary structure of proteins. In small model compounds and peptides, hydrogen atoms bound to carbon exchange very slowly or not at all at reasonable temperatures and *p*H, whereas hydrogens bound to oxygen or nitrogen exchange rapidly with hydrogen in the solvent. Peptide hydrogen atoms bound to nitrogen in proteins frequently exhibit a slower rate of exchange with solvent hydrogens than small peptides. This slower rate is ascribed to hydrogen bonding of the hydrogens or to their inaccessibility in a hydrophobic core of proteins (*1*).

Under more extreme conditions of temperature and acidity, carbon-bound hydrogens may also exchange with solvent protons. In a study of tritium exchange of proteins and amino acids in 6*N* HCl at 105°C for about 24 hours, up to two carbon-bound hydrogens of tyrosine exchanged with solvent protons (*2*). These investigators assigned the exchangeable hydrogens to the methylene group of tyrosine. Though this assignment is that expected for base-catalyzed exchange, it seemed unlikely for acid-catalyzed exchange. For this reason we studied the exchange of tyrosine hydrogens in DCl solutions at 100°C by proton-magnetic-resonance spectroscopy. In 18 hours we found no noticeable exchange of the methylene hydrogens but observed exchange of one of the two pairs of hydrogens attached to the aromatic carbons.

The proton-magnetic-resonance spectra were recorded on a Varian A60 spectrometer at room temperature. Chemical shifts are recorded as τ values with tetramethylsilane as an external standard. Tau values are obtained by subtracting the chemical shift in parts per million from the value of 10.0 assigned to tetramethylsilane. Higher τ values correspond to higher fields, and all tyrosine peaks appear toward the low-field side of the tetramethylsilane peak. No magnetic susceptibility corrections have been applied.

The spectrum of 0.3*M* tyrosine in 2.4*N* DCl consists of an apparent doublet centered at 6.7 τ, a triplet centered at 5.6 τ, and a complex A_2B_2 pattern with centers at 3.0 and 2.7 τ. From their position and spin-spin splitting patterns, the two high-field bands are assigned to aliphatic CH_2 and CH groups, respectively. On expanded scale these two high-field bands appear as a deceptively simple three-spin system (*3*) with an average coupling constant of 7.0 cy/sec.

By analogy with other results (*4*), the aromatic hydrogens at 3.0 τ are assigned to the pair *ortho* and those at 2.7 τ (lowest field) to the pair *meta* to the hydroxyl group on the benzene ring of tyrosine. These last two groups of protons are spin-spin coupled, and they give rise to the A_2B_2 pattern.

After heating the DCl solution of tyrosine for about 18 hours at 100°C, the proton-magnetic-resonance spectrum at room temperature was similar to that recorded above, except that the peaks centered at 3.0 τ had disappeared. Only a singlet appeared at 2.7 τ for the pair of aromatic hydrogens in the *meta* position to the hydroxyl group. No other changes due to heating were observed in the spectrum.

The results indicate that neither the aliphatic CH_2 or CH protons undergo exchange, after about 18 hours at 100°C, with deuterium in the acidic solvent. Disappearance of the complex A_2B_2 pattern and appearance of a sharp singlet at the lowest-field position after heating demonstrates that the high-field pair of aromatic protons has undergone exchange. From the chemical-shift analysis the pair of hydrogens that exchanged with deuterium of the solvent is in a position *ortho* to the hydroxyl group of tyrosine.

Hydrogen isotope exchange of *p*-cresol in aqueous sulfuric acid solutions has been determined gravimetrically by Gold and Satchell (*5*), who stated, "it seems legitimate to assume that the two nuclear positions concerned in the exchange are those *ortho* to the hydroxyl group." The chemical-shift analysis of our proton-magnetic-resonance study permits separate identification of each type of hydrogen environment and establishes that exchange does indeed occur predominantly in positions *ortho* to the hydroxyl group in *p*-substituted phenols. Possible mechanisms for the acid-catalyzed exchange have been discussed (*5, 6*).

R. BRUCE MARTIN
VITO J. MORLINO
*Cobb Chemical Laboratory,
University of Virginia, Charlottesville*

References and Notes

1. R. B. Martin, *Introduction to Biophysical Chemistry* (McGraw-Hill, New York, 1964), p. 245.
2. J. Hill and S. J. Leach, *Biochemistry* **3**, 1814 (1964).
3. R. J. Abraham and H. J. Bernstein *Can. J. Chem.* **39**, 216 (1961).
4. See, for instance, assignments for thymol, number 270, or 4-methyl-2-*t*-butylphenol, number 288 in Varian NMR Spectra catalog (1962).
5. V. Gold and D. P. N. Satchell, *J. Chem. Soc.* **1955**, 3609 (1955).
6. A. J. Kresge and Y. Chiang, *J. Amer. Chem. Soc.* **83**, 2877 (1961).
7. Supported by a grant from the National Science Foundation.

15 July 1965

Radiolysis of Estrone and Estradiol

Abstract. *Gamma irradiation of estrone and estradiol in 1*N *aqueous sodium hydroxide results in the formation of 2-hydroxyestrone and 2-hydroxyestradiol, respectively. Estrolactone (16a-oxa-D-homoestrone) was not encountered.*

Keller and Weiss (*1*) reported that the only product formed in the x-ray radiolysis of estrone in aqueous sodium hydroxide was a low (2-percent) yield of estrolactone. The radiolysis of aromatic compounds in aqueous solution usually leads to the formation of phenols.

Estrone was irradiated in 1*N* sodium hydroxide with cobalt-60 γ rays,